Experimental Study of Droplet Evaporation in a High-Temperature Air Stream

M. Renksizbulut[1]

M. C. Yuen

Professor and Chairman.
Mem. ASME

Department of Mechanical and
Nuclear Engineering,
Northwestern University,
Evanston, Ill. 60201

Heat transfer rates to simulated and freely suspended liquid droplets were measured in an atmospheric hot air tunnel. The experiments were limited to water, methanol, and heptane droplets in a Reynolds number range of 25 to 2000, and a mass transfer number range of 0.07 to 2.79. The present experimental data together with data by others can best be correlated by $Nu_f(1+B_f)^{.7}=2+0.57\ Re_M^{1/2}\ Pr_f^{1/3}$, where properties are evaluated at film conditions except for the density in the Reynolds number which is the free-stream density. Thus the data shows that at higher temperatures, evaporation reduces heat transfer rates directly by a factor of $(1+B_f)^{.7}$. Indirectly, evaporation affects heat transfer rates through the changes in both the composition and temperature of the surrounding gaseous medium.

1 Introduction

The importance of the study of heat and mass transfer of evaporating liquid droplets needs no introduction. The knowledge acquired is essential to the understanding and the prediction of the performance of a liquid spray. Much work has been done in the past. The majority of the work is, however, concentrated in low temperature environments. For heat and mass transfer of droplets in a low-temperature environment, the most recent review is found in a book by Clift, Grace, and Weber [1].

In a high-temperature environment, due to evaporation, the liquid remains at the wet-bulb temperature which is usually considerably lower than the free stream temperature. Under this circumstance, the driving potential for evaporation is the temperature gradient. In quasi-steady evaporation, the evaporation rate is the heat transfer rate divided by the heat of evaporation. Thus, heat and mass transfer are energetically synonymous. We shall follow the literature to consider only the heat transfer rate.

From the previous work of Eisenklam, Arunachalam, and Weston [2], Yuen and Chen [3], Harpole [4] and others, a clear picture of the effect of evaporation on heat and mass transfer emerges. Physically, the mass flux from evaporation dynamically affects the flow field surrounding the droplet. Energetically, evaporation causes large temperature gradients and changes the chemical composition; both directly affect the fluid properties adjacent to the droplets. Together, these effects can significantly alter the heat and mass transfer processes. The effect of mass flux is usually taken into account by the use of the mass transfer number, B. The variable properties effect can be taken into account by either the reference state method or the use of a correction factor.

Due to experimental difficulty, heat transfer data of evaporating droplets at high temperatures are rather scarce and individual investigators tend to correlate their own data.

In the reference state method, the reference temperature and mass fraction are defined as

$$T_r = T_d + r(T_s - T_d) \tag{1}$$

$$X_r = X_d + r(X_s - X_d) \tag{2}$$

where the value, r, varies from 0 to 1, depending on the particular reference state. For example, $r=0.5$ refers to the widely used film condition which is often denoted by the

subscript f in the heat transfer literature. The mass transfer number, B, is defined as

$$B_r = \bar{B}_r(1 + Q_R/Q_c) \tag{3}$$

where $\bar{B}_r$ is equal to $C_{pr}(T_s - T_d)/L_d$.

Early measurements of heat transfer rates were performed by Spalding [5] on various hydrocarbons in air with Reynolds numbers in the range from 800 to 4000 and B from 0.6 to 5. The correlation was found to be

$$Nu\ B_f^{2/5} = .53\ Re^{1/2}\ Pr \tag{4}$$

where the thermophysical properties are those of air at 20°C except for B_f.

Downing [6] carried out extensive measurements on suspended droplets of water, acetone, benzene and n-hexane in laminar air jets where temperatures ranged from 27°C to 340°C, Re ranged from 24 to 325 and the mass transfer number ranged from 0 to 2. The correlation of data is

$$Nu\ G = [1 - 0.4(1 - T_s)][2 + 0.6\ Re^{1/2}Pr^{1/3}] \tag{5}$$

where $G = \{[1 - 0.4(1 - B^{-1}ln(1+B))]B^{-1}ln(1+B)\}^{-1}$. The properties are evaluated at a reference state of $r = 0.6$.

Evaporation of water and other hydrocarbon droplets in high-temperature (up to 1000°C) air streams was reported in [2]. The Reynolds numbers varied from .01 to 15 and the mass transfer numbers from 0 to 3. The correlation is

$$Nu_f(1 + B_f) = 2 + 1.6\ Re_f^{1/2} \tag{6}$$

where the properties are evaluated using the film conditions ($r = 1/2$).

Narasimhan and Gauvin [7] investigated the evaporation of water from porous Celite spheres in superheated steam at temperatures from 500 K to 1000 K. The correlation is shown to be

$$Nu_f(1 + B_f)^{2/3} = .68\ Re_s^{1/2} \tag{7}$$

More recently, evaporation rates of water and methanol droplets were measured in a vertical air tunnel with temperatures up to 1000°C as shown in [3]. The Re varied from 200 to 2000 and B from 0 to 0.5. The correlation was shown to be

$$Nu_f[1 + B_f] = 2 + 0.60\ Re_M^{1/2}Pr_f^{1/3} \tag{8}$$

where Re_M is defined as $\rho_s u_s d/\mu_f$.

Theoretically, the problem of flow past an evaporating sphere at finite Reynolds numbers where both the effects of blowing and variable properties are considered is yet to be solved. Recently, Harpole [4] obtained the solution for evaporation at an axisymmetric stagnation point where both

the blowing and variable properties were taken into account. He then claimed that these effects for a sphere and a stagnation point are the same. Therefore, the solution for a sphere with evaporation is the solution for a sphere of constant property without evaporation multiplied by the ratio of the stagnation point solution with and without evaporation. In his solution for the stagnation point flow, the variable property effects are presented by correction factor method in contrast to the common usage of the reference state method. He claims that his solution agrees well with available experimental data.

It is quite apparent from the above discussion that the existing correlations pertinent to large temperature and concentration gradients exhibit considerable differences in their treatment of evaporation and variable property effects. The present study is therefore an extension of our earlier work at Northwestern University [3] to a wider range of mass transfer numbers and Reynolds numbers, and an attempt for a general correlation to incorporate all the existing available data.

2 Experiment

The present experiment is a continuation of [3] which is described in detail in [8] and will not be repeated here. Instead we shall only give a brief summary.

The experimental set-up is shown schematically in Fig. 1. The vertical wind tunnel has a contraction ratio of 13 to 1 and is capable of providing air velocities up to 20 m/s and temperatures up to 1000°C in the test-section. The heating elements are powered by d-c welders and consist of Inconel 601 strips which are arranged to act as flow straightener as well.

The test section is 36-cm long and has a 76×76-mm^2 cross-sectional flow area. Two of the side walls are made up of Vycor glass for observations and the other two are brick. Free stream and wall temperatures can be measured at three stations by using 50 μm platinum $-$ 13 percent rhodium traversing thermocouples and air velocities can be determined by using a Pitot tube. In turbulence measurements carried out at room temperature with a hot wire anemometer, it was found that, in the velocity range of the present measurements, the free-stream flow remained uniform with a turbulence intensity less than one-third of 1 percent within the 50×50-mm^2 core area of the test section.

The liquid feed line from the syringe pump to the droplet suspension tube is protected from the high-temperature air stream by a water-cooled housing and an elbow. The syringe pump is a high precision positive displacement injector which
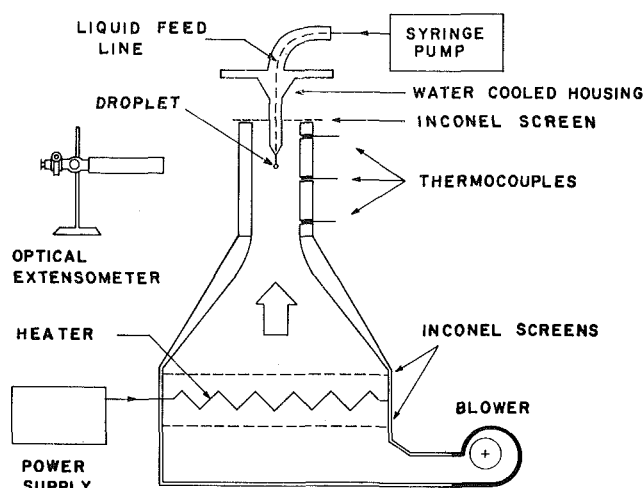

Fig. 1 Schematic of the experimental set-up

through a combination of different syringe sizes, a variable speed d-c motor and a gear box can supply flow rates in the range from 1.32×10^{-5} to 0.64 cm^3/s. The optical extensometer used for droplet size measurements provides 20X magnification at a working distance of 40 cm with 2.5-μm resolution.

Three methods are used to simulate the droplets depending on flow rate and the kind of liquid. The first method is to use a porous bronze sphere of 6.35-mm dia, with a thin liquid layer coating the surface of the sphere as in [3]. This is used in the Reynolds number range of 200 to 2000. The second method is to use a perforated brass sphere of 1.58-mm dia. This is used in the Reynolds number range of 50 to 500. The third method is to have a free liquid droplet suspending at the end of a capillary tube of 250-μm dia. This method is applicable to water droplets below Reynolds number of 200.

In the measurement of evaporation rate, the steady-state approach is used. Steady state is reached when the drop size remains constant (free droplet) or the liquid layer on the drop surface (porous or perforated sphere) remains uniform for a sufficient period of time. In this case the rate of liquid supply to the droplet must be equal to the evaporation rate.

In a typical experiment, the velocity and the temperature of the air stream in the test section were first brought into the range of preselected values by adjusting the power inputs to the wind tunnel blower and heater. Because of the large thermal inertia of the system, this process took over 3 hrs to complete when the wind tunnel was originally at room

--- Nomenclature ---

$a = (M_a/M_v)^n$
$A =$ parameter used in equation (11)
$B = \bar{B}(1 + Q_R/Q_c)$, mass transfer number
$\bar{B}, = C_p(T_s - T_d)/L_d$, mass transfer number without radiation heat transfer
$C_p =$ heat capacity
$d =$ diameter of droplet
$E =$ parameter used in equation (14)
$h =$ heat-transfer coefficient, enthalpy
$k =$ thermal conductivity
$L =$ latent heat of vaporization per unit mass
$M =$ molecular weight

$\dot{m} =$ mass flux
$n =$ constant
Nu $= hd/k$, Nusselt number
$p =$ parameter used in equation (11)
Pr $= C_p \mu/k$, Prandtl number
$Q =$ heat transfer
Re $= \rho u d/\mu$, Reynolds number
Re$_M = \rho_s u_s d/\mu_f$
$T =$ temperature
$\Delta T = (T_s - T_d)$, temperature difference
$u =$ velocity
$X =$ mass fraction
$Z =$ defined in equation (11)

Greek Symbols

$\alpha = \ln[(\rho k)_s/(\rho k)_d]/\ln(T_d/T_s)$

$\epsilon =$ emissivity
$\sigma =$ Stephan-Boltzmann constant
$\rho =$ density
$\mu =$ viscosity coefficient

Subscripts

$a =$ air
$c =$ convection
$d =$ droplet surface
$e =$ tube entrance
$f =$ film reference state
$l =$ liquid
$R =$ radiation
$r =$ reference state
$s =$ free stream
$t =$ tube
$v =$ vapor
$w =$ wall

temperature, and about 30 min between successive observations. Next, the water-cooled suspension probe was lowered into the test section until the droplet was approximately 8 cm from the exit plane. Subsequently, the test-liquid supply rate was monitored by changing the speed of the syringe pump while the droplet diameter was measured repetitively (with the optical extensometer), size variations being corrected through adjustments on the pump. Eventually, the desired steady state was reached when the droplet size remained fixed, and thus the rate of liquid supply by the pump was equal to the rate of evaporation. As a rule, a record of the observation was made only when steady-state evaporation persisted for at least 2 min. Thermocouple, pressure transducer, and pump readings were then registered completing the process.

For interpretation of the experimental data, the steady-state energy equation is applied to the control volume as shown in Fig. 2.

$$Q_c + Q_R = \dot{m}L_d + \dot{m}[h_l(T_d) - h_l(T_e)] - (Q_t + Q_l) \qquad (9)$$

where Q_c and Q_R are the convective and radiative heat flux to the drop, $\dot{m}$ is the mass flux, L_d is the latent heat, h_l is the enthalpy of the liquid, T_d is the drop surface temperature, T_e is the liquid temperature at the end of the tube, Q_t and Q_l are the heat loss or gain from the tube and liquid in the tube. An order of magnitude analysis has shown that the last term in equation (9) is negligible [8].

The values of wet-bulb temperature (T_s) as a function of free-stream temperatures are listed in Table 1. These wet-bulb temperatures are taken from Yuen and Chen [9]. In the case of the porous sphere, T_e was measured and was found to have a maximum deviation of 4°C from T_d. For smaller droplets (perforated sphere and suspended droplets), it was assumed that T_e was equal to T_d. The effect of natural convection in this case has been estimated in reference [8] to be negligible. Thus, Q_c in equation (9) represents only heat transfer from forced convection.

Wall temperatures in the test section were maintained essentially uniform by placing an Inconel screen at the channel exit. For isothermal walls at a temperature, T_w, surrounding the droplet, the thermal radiation can be computed from

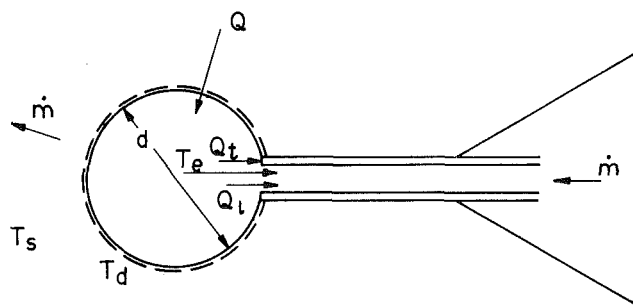$$Q_R = \pi d^2 \, \sigma \, \epsilon [T_w^4 - T_d^4] \qquad (10)$$

Fig. 2 Schematic diagram of an evaporating droplet

where σ is the Stephan-Boltzmann constant and the emissivity, ϵ, of the liquid is assumed to be 0.95 and equal to absorptivity. A more accurate formulation of the radiation problem using shape factors and appropriate emissivities (e.g., $\epsilon = 0.85$ for Vycor and 0.65 for refractory brick walls) for the surfaces involved is given in detail in [8]. The result shows that equation (10) can predict Q_R to within 4 percent. The physical reason is that in an enclosure, the net result of interreflections is to make the wall radiosity more nearly that of a black body. For most of the present experimental data, Q_R is much less than 1/3 of Q_c.

3 Results and Discussion

Heat transfer rates of water, methanol, and n-heptane droplets at atmospheric pressure were measured with air stream temperatures up to 800°C. A total of 288 data points were recorded covering the range of variables summarized in Table 2. Other pertinent information for each of the data points can be found in [8].

Following [3], it was found that the data can be correlated in the following form

$$Z^p \equiv [\mathrm{Nu}(1+B)^p - 2]\mathrm{Pr}^{-1/3} = A\,\mathrm{Re}^{1/2} \qquad (11)$$

For $\mathrm{Re} \to 0$ and negligible evaporation $(B \to 0)$, equation (11) approaches the theoretical limit of $\mathrm{Nu} = 2$, provided that free convection can be neglected. Furthermore, for small temperature differences between the droplet and the free stream $(B \to 0)$, equation (11) agrees with the correlation of Ranz and Marshall [10] if A equals 0.6. In the present study, the Prandtl number varied between 0.7 and 1. Hence, the difference between $\mathrm{Pr}^{1/3}$ and $\mathrm{Pr}^{0.38}$ as proposed by [4] has negligible effect on the overall correlation. What remains to be determined in equation (11) is the proper reference state to evaluate the thermodynamic and transport properties in the dimensionless numbers and the exponent p.

Table 1 Wet-bulb temperatures and mass transfer numbers as a function of free-stream temperatures.

$T_s(°C)$	$T_d(°C)$	$\bar{B}_f$
	Water	
100	33	0.028
200	50	0.067
400	71	0.061
600	84	0.267
800	90	0.415
	Methanol	
100	26	0.067
200	45	0.16
400	55	0.42
600	60	0.74
	n-Heptane	
100	36	.20
200	55	.56
400	75	1.75
600	90	3.62

Table 2 Experimental range of variables

Test liquid	Water	Methanol	n-Heptane	All data
Data size	120	81	87	288
T_s, (°C)	204-786	193-485	238-450	193-786
ΔT, (°C)	154-696	149-427	178-371	149-696
u_s, (m/s)	0.8-5.1	0.9-9.0	1.4-8.6	0.8-9.0
d, (mm)	0.9-2.12	1.62-6.35	1.64-6.35	0.92-6.35
Re_M	24-201	58-1788	78-1974	24-1974
B_f	0.07-0.46	0.16-0.64	0.9-2.79	0.07-2.79
$(Q_R/Q_C)_{max}$	0.173	0.221	0.340	0.340

According to [3], the best correlation of experimental data following equation (11) is

$$Z_f^{1.0} = [\mathrm{Nu}_f(1 + B_f) - 2]\mathrm{Pr}_f^{-1/3} = 0.60 \, \mathrm{Re}_M^{1/2} \qquad (12)$$

where the exponent p is 1, A is 0.60 and $\mathrm{Re}_M = \rho_s U_s d/\mu_f$. The subscript f denotes the film condition as defined in equations (1) and (2) with $r = 1/2$.

The present experimental data are shown in Fig. 3 together with equation (12). Figure 3 shows that the water and methanol data agree well with equation (12); the heptane data, however, are consistently higher. The correlation of equation (12) was based on water and methanol data in [3], where the maximum B number was about 0.5. Therefore the correlation was not sensitive to the exponent p.

One of the primary purposes of the present experimental investigation is to extend the range of Re and B in order to further test the validity of equation (12). It now appears that equation (12) does not correlate well with data where the B number is higher than one. The new experimental results show that the best correlation of the data is

$$Z_f^{0.70} \equiv [\mathrm{Nu}_f(1 + B_f)^{0.70} - 2]\mathrm{Pr}_f^{-1/3} = 0.57 \, \mathrm{Re}_M^{1/2} \qquad (13)$$

The uncertainties associated with $A = 0.57$ and $p = 0.70$ are ± 0.032 and ± 0.062, respectively. The latter standard

deviation is based on data points with $B_f > 0.15$. Equation (13) together with the experimental data are plotted in Fig. 4.

The use of two different reference states for the Reynolds number $(\mathrm{Re}_M = \rho_s u_s d/\mu_f)$ is perhaps inconvenient but
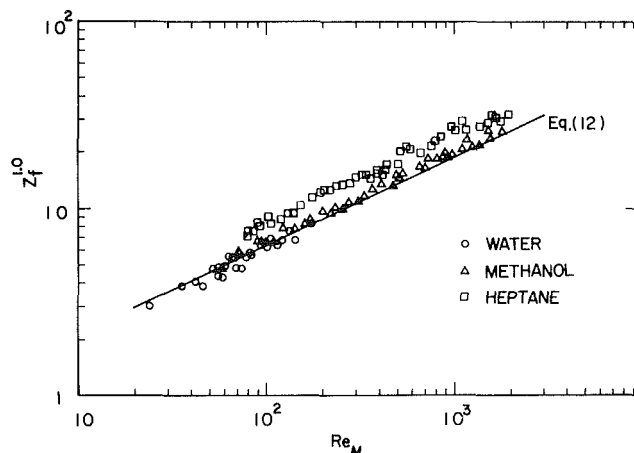

Fig. 3 Correlation of present heat transfer rates of evaporating liquid droplets in air according to [3]
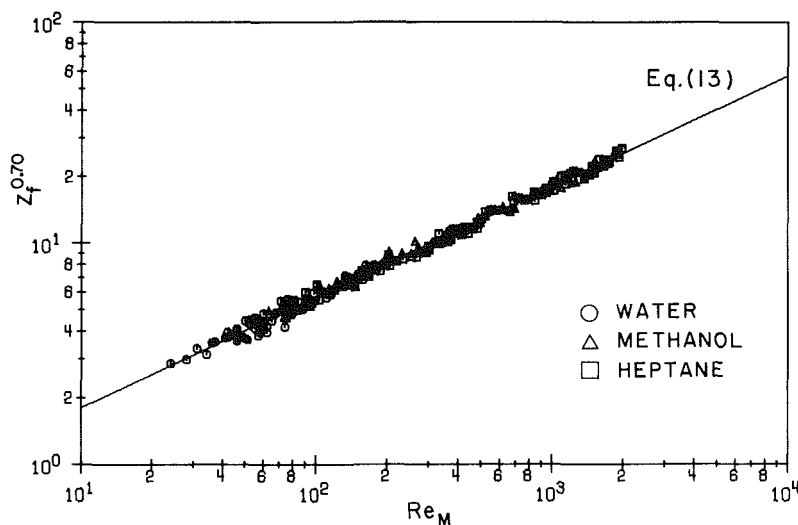

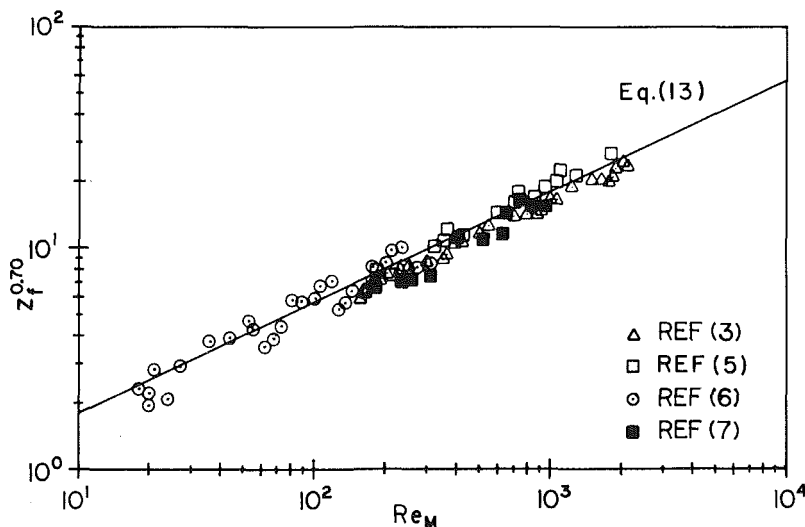Fig. 4 Improved correlation of present heat transfer rates of evaporating liquid droplets in air

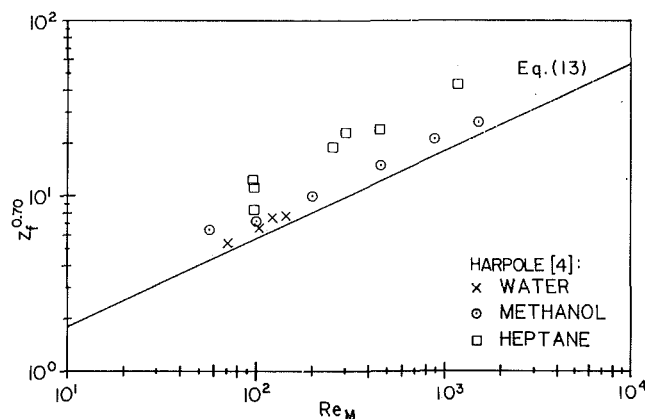Fig. 5 Comparison of present correlation with other experimental data

Fig. 6 Comparison of present correlation with Harpole's correlation [4]

physically justifiable if the Reynolds number is interpreted as a ratio of inertia to viscous forces. As shown in [3, 9] the inertia force is proportional to $\rho_s u_s^2$, and the viscous force is proportional to $\mu_r u_s/d$, where the viscosity should be evaluated using a reference state close to the body. In this case the film condition ($r=0.5$ in equations (1) and (2)) is appropriate.

In Fig. 5, the data of [3] are shown and the comparison with equation (13) appears to be satisfactory. The reason is that for relatively small values of B (less than 0.5) as in [3], the difference between $(1+B)^{0.7}$ and $(1+B)$ is only a few percent which is well within the experimental error. For further comparison, the data of [5, 6, 7] are also plotted in Fig. 5. They seem to agree satisfactorily with the new correlation of equation (13).

Harpole [4] has claimed that his calculation agrees well with the data of [3]. He used a multiplicative correction factor to take into account the effect of variable properties. Since the data of [3] agrees with equation (13) which includes a liquid of high molecular weight, it is useful to see if the calculation of Harpole agrees with equation (13). Equation (31) of [4] can be expressed as

$$\text{Nu}_s[1 + aB_s]^{.7} = E[1.56 + .626\text{Pr}_s^{38}\text{Re}_s^{1/2}] \tag{14}$$

where

$$E = [1 + (0.327\alpha - .0844)(1 - T_d/T_s)]$$

and

$$\alpha = ln[\rho k]_s / (\rho k)_d]/ln(T_d/T_s),$$

$$a = (M_a/M_v)^n$$

A detailed calculation shows that α varies from about 0.16 at low temperatures to about .22 at high temperatures. Thus, E is very close to 1. Therefore, any variable property effect due to both temperature and composition changes is represented by "a" which is the ratio of the molecular weights of air and liquid vapor to the power n.

In equation (14), Re_s is the free-stream Reynolds number which for the same free-stream condition is larger than Re_M in equation (13). For the same rate of convective heat transfer, Nu_f is much larger than Nu_s because k_s/k_f is larger than 1. Thus dividing equation (14) by equation (13) we have

$$\frac{\text{Nu}_s}{\text{Nu}_f}\left(\frac{\text{Re}_M}{\text{Re}_s}\right)^{1/2} \approx \left[\frac{1+\bar{B}_f}{1+aB_s}\right]^{.7} \tag{15}$$

Since the left-hand side of equation (15) is always less than 1,

that means $aB_s > \bar{B}_f$. Again, a detailed calculation shows that $B_s < \bar{B}_f$ and therefore "a" has to be larger than 1. This is certainly not true when the molecular weight of the liquid is much larger than that of air as in the case of heptane.

Although in [4] the author mentioned that "a" is equal to M_a/M_v raised to a certain power, but in effect, in the case of water droplets, the author used $a = 1.6$ which is the ratio of the molecular weights to the first power. Data obtained from equation (14) after assuming $a = M_a/M_v$ are compared with equation (13) in Fig. 6. The predictions of equation (14) do not correlate with equation (13) as shown in Fig. 6. In particular, the heptane results disagree significantly with the new experimental correlation. The data of water and methanol agree better with equation (13). Part of the discrepancy is due to the predicted wet-bulb temperatures of water droplets which are systematically lower than the experimental values as listed in Table 1. However this cannot completely account for the disagreement. Apparently both the temperature and composition variation change the properties in a more complicated fashion than that indicated by the simple correction factor "a" (ratio of the molecular weights).

4 Conclusion

The present investigation shows that Nusselt numbers for single component droplets evaporating in high-temperature air streams can be accurately predicted by equation (13). In a low-temperature environment, equation (13) reduces to essentially the standard heat transfer equation of Ranz and Marshall [10]. At a high-temperature environment, the present correlation shows that evaporation reduces heat transfer rates directly by a factor of $(1+B_f)^{.70}$. Indirectly evaporation affects heat transfer rates through changes in both the temperature and composition of the surrounding gaseous medium. This effect is accounted for by evaluating the thermophysical properties at the film conditions provided that the definition of Reynolds number is based on the free stream mass flux $\rho_s u_s$.

References

1 Clift, R., Grace, T. R., and Weber, M. E., *Bubbles, Drops and Particles*, Academic Press, New York, 1978.

2 Eisenklam, P., Arunachalam, S. A., and Weston, J. A., "Evaporation Rates and Drag Resistance of Burning Drops," *Eleventh International Symposium on Combustion* 1967, pp. 715-727.

3 Yuen, M. C., and Chen, L. W., "Heat Transfer Measurements of Evaporating Liquid Droplets," *International Journal of Heat and Mass Transfer*, Vol. 21, 1978, pp. 537-542.

4 Harpole, G. M., "Droplet Evaporation in High Temperature Environments," ASME JOURNAL OF HEAT TRANSFER, Vol. 103, 1981, pp. 86-91.

5 Spalding, D. B., "Experiments on the Burning and Extinction of Liquid Fuel Spheres," *Fuel*, Vol. 32, 1953, pp. 169-185.

6 Downing, C. G., "The Evaporation of Drops of Pure Liquids at Elevated Temperatures, Rates of Evaporation and Wet-Bulb Temperatures," *AIChE Journal*, Vol. 12, 1966, pp. 760-766.

7 Narashimhan, C., and Gauvin, W. H., "Heat and Mass Transfer to Spheres in High Temperature Surroundings," *Can. J. Chem. Eng.*, Vol. 45, 1967, pp. 181-188.

8 Renksizbulut, M., "Energetics and Dynamics of Droplet Evaporation in High Temperature Intermediate Reynolds Number Flows," Ph.D. dissertation, Northwestern University, 1981.

9 Yuen, M. C., and Chen, L. W., "On Drag of Evaporating Liquid Droplets," *Combustion Science and Technology*, Vol. 14, 1976, pp. 147-154.

10 Ranz, W. E., and Marshall, W. R., "Evaporation from Drops: I, II," *Chemical Eng. Progress*, Vol. 48, 1952, pp. 141-146, pp. 173-180.